IASMiRT

SMiRT 26
50 Anniversary Berlin/Potsdam

Transactions, **SMiRT-26**
Berlin/Potsdam, Germany, July 10-15, 2022
Special Session

PREDICTION OF PULL-OUT CAPACITY OF HEADED ANCHOR IN CONCRETE UNDER MONOTONIC AND CYCLIC LOADING USING COHESIVE ZONE MODELING

Minkwan Ju[1], Siwoo Jeon[2], Kyoungsoo Park[3]

[1] Research Professor, Yonsei University, Seoul, Republic of Korea (j_dean21@yonsei.ac.kr)
[2] Master Student, Yonsei University, Seoul, Republic of Korea (siwoo@yonsei.ac.kr)
[3] Associate Professor, Yonsei University, Seoul, Republic of Korea (k-park@yonsei.ac.kr)

ABSTRACT

A concrete anchor is typically utilized for placing the system equipment in the nuclear power plants (NPPs), and thus the assessment of the concrete anchor pull-out capacity is essential for the safety management of NPP under extreme environments like earthquake. However, the prediction of the concrete anchor pull-out capacity is extremely challenging especially under cyclic loading conditions because most design equations are based on the measured concrete strength in conjunction with a curve fitting process. In this study, the concrete anchor failure behaviour is predicted using the cohesive zone-based finite element analysis for cyclic loading conditions, which accounts for nonlinear fracture process of concrete. Concrete fracture characteristics such as the cohesive strength and fracture energy are measured using the three-point bending and indirect tension tests. Based on the measured material properties, the computational results well estimate the experimental concrete anchor failure behaviours.

INTRODUCTION

Concrete anchor is an effective method to make rigid body system between an equipment and a concrete member. Failure mechanism is typically governed by pull-out strength having cone failure shape due to the concrete tensile failure. Accordingly, the pull-out strength is the critical performance index for evaluating or predicting the concrete anchor system. The standard code equations have used considerable low strength reduction factors of 0.45 – 0.75 due to the uncertain structural behavior of anchor failure (ACI 318 2014, KDS 2021, Model Code 2010). To improve the highly conservative application, the more precise prediction of the pull-out strength is employed and utilized to the empirical equation update. There have been the finite element analysis using concrete damage model for the anchor pull-out behavior (Lu et al. 2019). In this study, concrete anchor specimens are fabricated and tested. The results are compared with the standard code equation for break out strength. For computational approach, crack growth analysis method by cohesive zone modelling is developed and applied to pull-out strength analysis. Furthermore, under cyclic loaning condition, a three-points bending specimens are employed to predict the load and displacement as well as the failure cycles estimation.

EXPERIMENTAL PROGRAM

Materials

The water to cement ratio (w/c) is 42.5 % and the design strength is 40 MPa. For the workability, a superplasticizer is applied. Table 1 shows the mixing proportions of this study.

Table 1: Mixing proportions.

W/C (%)	S/a (%)	Air (%)	Unit weight (kg/m^3)				
			Water	Cement	Sand	Gravel	Admixtures*
42.5	47	4.0	170	400	810	914	3.2 (0.8%)

* superplasticizer

Fabrication of Test Specimens

Anchor specimens are fabricated with the concrete block made of plain concrete with the size of 600 × 600 × 200 mm. There are 100 mm spacing holes at the edge side for specimen fixing to the test machine. Anchor steel is installed at the center of the concrete block with the embedment length of 70, 100, and 130 mm, respectively. The diameter of circular anchor and anchor steel are 50 mm and 16 mm, respectively. For vertical alignment of the anchor steel, there is the steel extension from the circular anchor to the bottom of the anchor block. To avoid the mechanical friction around the extension during the pull-out loading, the plastic bubble wrapping is applied. Figure 1 is about the geometry and Figure 2 is the fabrication process. There are three types of anchor installation varying embedment lengths. The number of specimens is two for each replicate. Additionally, cylindrical specimens are fabricated to measure the compressive strength of concrete, and the averaged compressive strength is 40.6 MPa. Table 2 shows the test variables in this study.

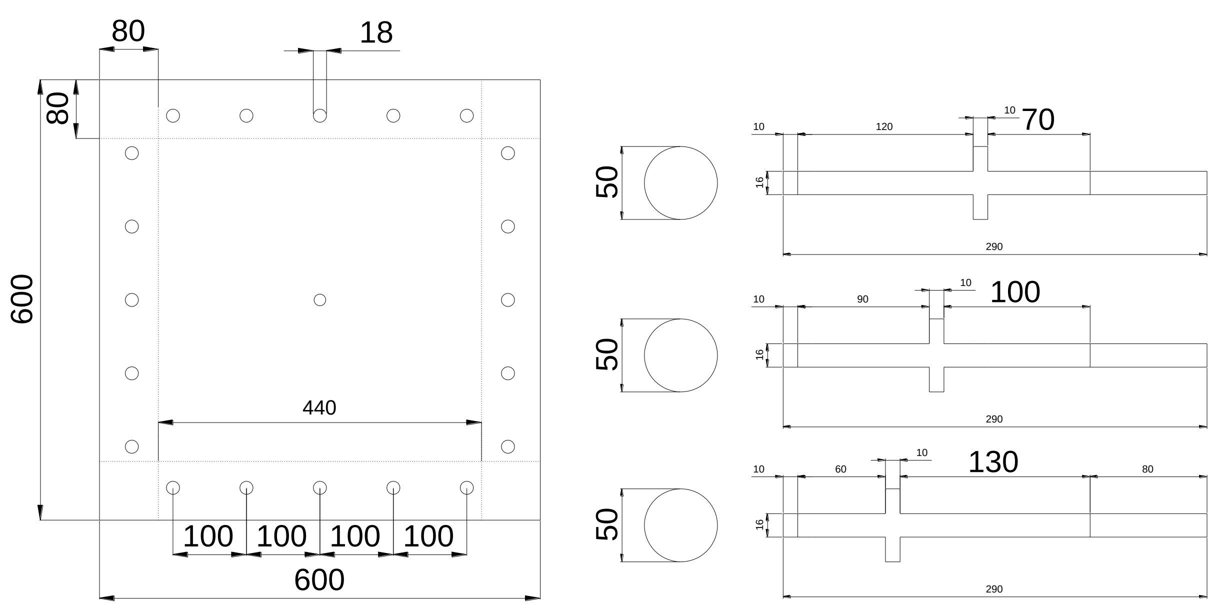

Figure 1. Geometry of anchor pull-out test specimen and details of anchor steel.

Figure 2. Fabrication process of the concrete anchor specimens.

Table 2: Test variables for the anchor pull-out tests.

Specimen ID	Anchor bolt dia. (mm)	Anchor bolt head dia. (mm)	h_{ef} (mm)	f_c' (MPa)	# of anchor specimens
A16-70			70		2
A16-100	16	50	100	40.6* ± 2.1	2
A16-130			130		2

* average compressive strength

Experimental Test

The pull-out loading is vertically applied to the anchor steel using MTS 810 with the capacity of 250 kN as shown in Figure 3. The specimen is fixed with the testing jig at the bottom level using high tension bolts along the four edges. To completely obtain the load and displacement curves, the loading rate is adopted with 0.05 mm / min under the displacement control and it can measure the softening behaviour. There are five cylinders of Ø100×200 mm for measuring the compressive strength and the indirect tensile strength according to ASTM C469 and ASTM C496, respectively.

Figure 3. Test setup for the anchor pull-out test.

EXPERIMENTAL TEST RESULTS

Mode of Failure

Two types of failure mode are observed: concrete cone failure and concrete splitting failure. The former is usually shown in smaller embedment length: the latter is for the longer one. The cone failure is subjected to the edge failure when the crack propagation is stop at the fixed steel plates.

Figure 4. Cone failure of concrete.

Load and Displacement Behavior

Figure 5 presents the load and displacement behaviour of the test specimens. The initial stiffness is all similar among each other based on the relatively small deviation in the compressive strength and the tensile strength of concrete. For the peak load, A16-70 samples have much less peak load than A16-100 and A16-130 samples. After peak load, the load largely drops due to the concrete cracking failure and this trend is much clear for A16-100 and A16-130 samples. This is because the deeper embedment length in concrete has high cracking resistance energy and it is rapidly released after cone failure or concrete splitting failure.

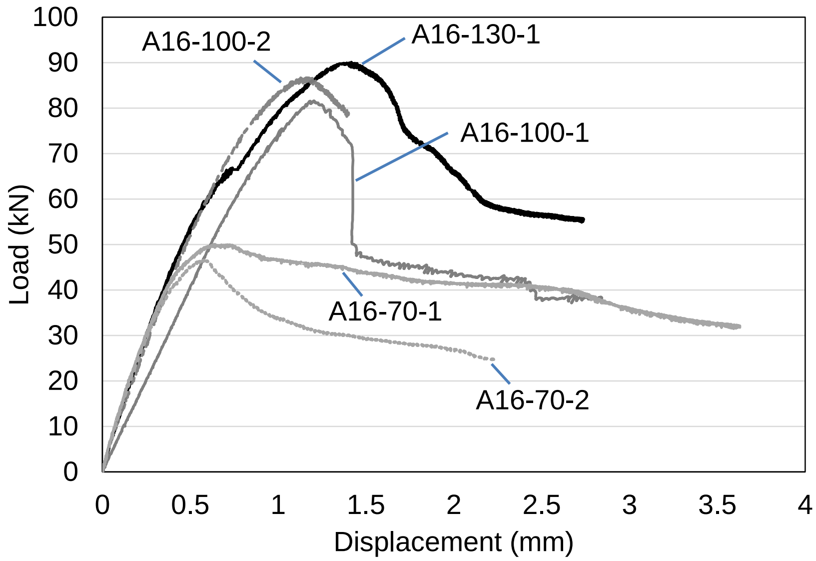

Figure 5. Monotonic load and displacement curves

Comparison of Experimental Strength with Design Code

To analytically evaluate the pull-out strength of test specimens, ACI 318 design code equation is used as;

$$N_b = k_c \lambda_a \sqrt{fc'} h_{ef}^{1.5} \tag{1}$$

$$N_u = \frac{A_{Nc}}{A_{Nco}} \Psi_{ed,N} \Psi_{c,N} \Psi_{cp,N} N_b \tag{2}$$

where k_c = coefficient for basic breakout strength in tension (For cast-in-anchor, 24), λ_a = lightweight concrete coefficient (For normal weight, 1.0), $\Psi_{ed,N}$ = factor used to modify tensile strength of anchors based on proximity to edges of concrete member (For edge distance > 1.5h_{ef}, 1.0), $\Psi_{c,N}$ = factor used to modify tensile strength of anchors based on presence or absence of cracks in concrete (For cast-in-anchor, 1.25), $\Psi_{cp,N}$ = factor used to modify tensile strength of post installed anchors intended for use in uncracked concrete without supplementary reinforcement to account for the splitting tensile stresses due to Installation (For cast-in-anchor, 1.0)

Table 3 summarizes the measured pull-out strength, the nominal strength of ACI-318, and the ratio of the measured to nominal strength. The ratios are ranged within 1.01 – 1.16. The results show good corresponding prediction, however, the cone failure is governed not in free surface but in the fixed steel plate. Thus, this situation may affect the experience the premature failure of the test specimens.

Table 3: Measured concrete pull-out strength.

Test specimens	Pull-out strength (kN)			Test to predicted ratio (Average / ACI-318)
	Measured	Average	ACI-318	
A16-70	46.8 / 50.0	48.4 ± 1.6	46.5	1.01
A16-100	81.6 / 86.9	84.3 ± 2.7	79.5	1.06
A16-130	94.2 / 124.4	109.3 ± 15.1	94.2	1.16

Cyclic Loading using Cohesive Zone Modeling

The cohesive zone model (CZM) is generally employed to represent nonlinear fracture process of quasi-brittle materials like concrete (Bazant and Planas, 1998; Park and Paulino, 2011). Recently, Choi and Park (2019) developed a computational method to remove mesh bias in CZM in conjunction with the stress recovery technique (Choi et al., 2022), and Choi et al. (2020) proposed a mixed-mode fatigue crack growth model in conjunction with the potential-based cohesive zone model (Park et al., 2009). In order to validate the proposed concrete crack growth model, experimental results by Shah and Kishen (2012) were employed in this study. The cyclic test of a concrete beam was configured shown in Fig. 6. The cyclic loading was applied with 0.5 kN / 500 cycles and the constant minimum load was 0.2 kN. The compressive strength of concrete was 34 MPa, and the peak load from the monotonic loading test was measured as 4.46 kN. The elastic modulus and the Poisson′s ratio are 21 GPa and 0.25, respectively.

For the fracture parameters, the cohesive strength was 4.6 MPa and the fracture energy was 150 N/m and the shape parameter was 5. The fatigue separation and traction resistance parameters were used with 250 and 1,650, respectively and the contact separation ratio was 0.3. For the monotonic loading test, the peak load was similar with the computational peak load of 4.46 kN. For the cyclic loading test, the load and crack mouth opening displacement (CMOD) are plotted in every 500 cycles up to 3,000 cycles and in every 100 cycles after 3,000 cycles including the last cycle before the failure, as shown in Fig. 7.

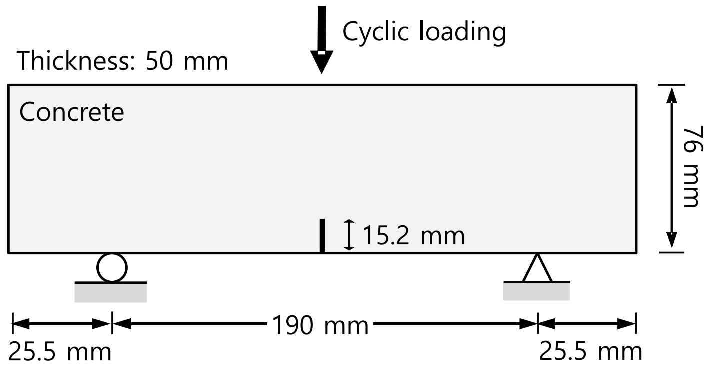

Figure 6. Three-point bending cyclic loading specimen.

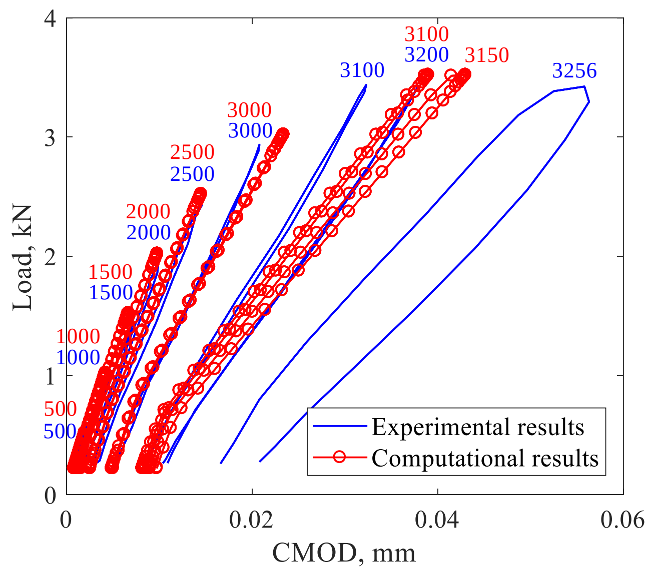

Figure 7. Fatigue crack growth analysis results (Choi et al. 2020).

CONOCLUSIONS

1) Anchor failures are resulted in two types of concrete cone failure and concrete splitting failure within the designated failure perimeter. It depends on the embedment length. Thus, the deeper length shows the higher peak load and cracking resistance.

2) The strength ratio of the measured to nominal one is in the range of 1.10 – 1.16, although the deepest one tends to have more underestimate prediction. These are mainly by the cracking failure at the fixed edges, hence, further experimental validations may be needed.

3) The cyclic computational and experimental results of the three-points bending tests demonstrate the decrease of the stiffness and the increase of a finite separation at the minimum load according to the cyclic loading. The failure cycles in computational are 3,256 cycles, while the experimental test is failed at 3,208 cycles. It is found that the developed fatigue crack growth model can give good prediction in low cyclic failure.

ACKNOWLEDGEMENT
The authors acknowledge the supports from the Basic Science Research Program through the National Research Foundation of Korea (NRF) funded by the Ministry of Science, ICT & Future Planning (grant number: 2022R1A2C2010081).

REFERENCES

ACI 318-14. (2014). *Building Code Requirements for Structural Concrete and Commentary*, American Concrete Institute, Farmington Hills, MI, USA.

ASTM C469. (2014). *Standard Test Method for Static Modulus of Elasticity and Poisson's Ratio of Concrete in Compression*. In ASTM International. ASTM International, West Conshohocken, PA, USA.

ASTM C496. (2017). *Standard Test Method for Splitting Tensile Strength of Cylindrical Concrete Specimens*. In ASTM International. ASTM International, West Conshohocken, PA, USA.

Bazant, Z., and Planas, J. (1998). *Fracture and Size Effect in Concrete and other Quasibrittle Materiales*. In CRC press LCC.

Choi, H., and Park, K. (2019). "Removing mesh bias in mixed-mode cohesive fracture simulation with stress recovery and domain integral," *International Journal for Numerical Methods in Engineering*, 120, 1047-1070.

Choi, H., Park, K. and Paulino, G.H. (2020). "Mixed-mode fatigue crack growth using cohesive zone modeling," *Engineering Fracture Mechanics*, 240, 107234.

Choi, H., Cui, H. and Park, K. (2022). "Evaluation of stress intensity factor for arbitrary and low-quality meshes using virtual grid-based stress recovery (VGSR)," *Engineering Fracture Mechanics*, 263, 108172.

Lu, J., Zhang, Y., Muhammad, H., Chen, Z., Xiao, Y. and Ye, B. (2019). "3D analysis of anchor bolt pullout in concrete materials using the non-ordinary state-based peridynamics," *Engineering Fracture Mechanics*, 207, 68-85.

KDS 14 20 54. (2021). *Design Standard of Concrete Anchor*. Ministry of Land, Infrastructure and Transport, Sejong, Korea.

Model Code 2010. (2010). *fib Model Code for Concrete Structures*, International Federation for Structural Concrete (fib), Lausanne, Switzerland.

Park, K. and Paulino, G.H. (2011). "Cohesive zone models: a critical review of traction-separation relationships across fracture surfaces," *Applied Mechanics Reviews*, 64(6).

Shah, S.G. and Kishen J.M.C. (2012). "Use of acoustic emissions in flexural fatigue crack growth studies on concrete," *Engineering Fracture Mechanics*, 87, 36-47.